J Mater Sci (2010) 45:1432–1437
DOI 10.1007/s10853-009-4089-0

INTERFACE SCIENCE

Effect of interface structures on the fracture behavior of two-dimensional carbon/carbon composites by isothermal chemical vapor infiltration

Yong-Gang He · Ke-Zhi Li · He-Jun Li · Jian-Feng Wei · Qian-Gang Fu · Dong-Sheng Zhang

Received: 22 July 2009 / Accepted: 25 November 2009 / Published online: 10 December 2009

Abstract The interface structures and fracture behavior of the two-dimensional carbon/carbon composites by isothermal vapor infiltration have been investigated. The results show that the graphene layers exhibit long-range order in high/textured pyrocarbon matrix and are curved in about 5-nm interface region of the fiber/high-textured. Some globular nanoparticles are formed on the fiber surface and the high-textured layer about 10 nm exists in the interface of the fiber/low-textured. The graphene layers stacks are scrolled and folded in the medium-textured and they are waved together in the interface of the fiber/medium-textured. The pseudo-plastic fracture behavior of the two-dimensional carbon/carbon composites is resulted from the dominant high-textured matrix and a moderate interfacial bonding force. A strong adhesion of the fiber/low-textured and the thicker fiber increased by surrounding low-textured layer result in the increasing flexural strength. The single medium-textured and a very strong bonding force of the fiber/medium-textured lead to the brittle fracture behavior.

Introduction

Carbon/carbon (C/C) composites have attracted extensive attentions due to their excellent mechanical properties at ultrahigh temperature, such as high specific strength, specific modulus, and steady strength above 2473 K [1, 2]. Therefore, they are suitable for aircraft and aerospace applications. The C/C composites are often fabricated by isothermal chemical vapor infiltration (ICVI) of porous carbon fiber preforms. Benzinger and coworkers [3–5] have investigated the correlation between ICVI process parameters and pyrocarbon matrix microstructures. Meanwhile, several models have been proposed to correlate the degree of texture in a qualitative way with the composition of the gas phase. The textures of the bulk pyrocarbon matrix could be controlled well by choosing appropriate ICVI process parameters. However, the texture of the very first layer of pyrocarbon about a few nanometers thick is considerably difficult to control. Furthermore, the structure and characteristics of the interface determine the adhesion between fiber and matrix. The mechanical properties of C/C composites tremendously depend on load transfer at fiber/matrix (F/M) interface. A weak interface may impair the integrity of composites, whereas a strong bond may induce brittle fracture behavior [6–8]. Therefore, study of interface characteristics is essential for the development of C/C composites with desirable and predictable behavior.

The two-dimensional carbon/carbon (2D C/C) composites are widely used as brake disks for airplane in aeronautic fields. It is well known that the microstructure of pyrocarbon matrix and the property of interface greatly affect their mechanical and tribological properties. A number of researchers have extensively studied the microstructure of pyrocarbon matrix and failure mechanism of C/C composites by ICVI [9–11]. However, the earlier study mainly focused on the structure and mechanical properties of the carbon fiber felts by ICVI. Although a few studies have been reported on the influence of the matrix texture on the fracture behavior of 2D C/C composites [12, 13], the structural properties of the F/M

Y.-G. He · K.-Z. Li (✉) · H.-J. Li · J.-F. Wei · Q.-G. Fu · D.-S. Zhang
Carbon/Carbon Composites Technology Research Center, Northwestern Polytechnical University, Xi'an, Shaanxi 710072, People's Republic of China
e-mail: likezhi@nwpu.edu.cn

Y.-G. He
e-mail: heyg@mail.nwpu.edu.cn

interface and their effect on the fracture behavior of 2D C/C composites by ICVI have not appeared yet in the literature.

In this study, the micro-and nanostructures of the F/M interface of 2D C/C composites by ICVI were analyzed systematically by high-resolution transmission electron microscopy. In particular, the effect of interface microstructures on the facture behavior of 2D C/C composite was discussed.

Experimental

Preparation of the 2D C/C composites

The investigated samples are 2D needle-punched fiber felt with a fiber volume fraction of 25% and a special architecture of 0°/90°/0°/90°. The PAN (polyacrylonitrile)-based carbon fibers forming the felts have a typical mean diameter of 7 μm. The fiber density is 1.72 g/cm^3. All the preforms were heat-treated at 1773–1973 K before densification to remove the impurity on the fiber surface. The infiltration was carried out by means of ICVI process using methane as precursor gas and nitrogen as the diluted gas at negative pressure. The experimental operation and infiltration procedure were described in detail in Ref. [14]. The infiltration conditions were adjusted to obtain bulk samples with different pyrocarbon matrix. Samples A and B were densified at 1373 K with the methane partial pressure of 10 and 20 kPa, respectively. Sample C was infiltrated at 1323 K with the methane partial pressure 30 kPa. The same gas residence time of 0.1 s was used for preparing the three samples. The bulk densities of the three samples were increased to 1.75 g/cm^3 by different densification time.

Characterization methods

The infiltrated 2D C/C composites were heated in high-temperature graphitization furnace at 2373 K for 2 h at an argon atmosphere. Three rectangular bars of 55 mm × 10 mm × 4 mm along the fiber layer direction were cut from the inner region of the samples A–C, respectively. Three-point bending tests were carried out in accordance with Q/GB95-92 on a CMT5304-30KN universal testing machine. The optical observation was performed on polarized light microscopy (PLM, Leica DMLP). The extinction angle (Ae) was measured according to the procedure described by Bourrat et al. [15]. Three kinds of the pyrocarbon can be distinguished: low-textured (LT, Ae $< 12°$), medium-textured (MT, $12° \leq$ Ae $< 18°$), and high-textured (HT, Ae $\geq 18°$). The morphologies of fracture surface and the textures of pyrocarbon matrix were examined by scanning electron microscopy (SEM, JSM-6700F). The microstructures of the F/M interface were analyzed by (high-resolution) transmission electron microscopy (TEM/HRTEM, JEM-3010) combining with selected area electron diffraction (SAED). The orientation angle (OA) is obtained by SAED patterns. According to Reznik and Hűttinger [16], the pyrocarbon textures are classified into LT, $80° \leq$ OA $< 180°$, MT, $50° \leq$ OA $<80°$, and HT, OA $< 50°$.

Results and discussion

Textures and microstructures of the interface

The polarized light micrographs of the samples A-C are shown in Fig. 1. The textures vary significantly with the changing of infiltration process conditions. The matrix of sample A infiltrated at 1373 K with the methane partial pressure of 10 kPa exhibits pure HT. The matrix of sample B densified at identical temperature with a higher methane partial pressure 20 kPa possesses double textures around the fiber. The inner dark layer about 1 μm thick is LT layer and the outer layer is HT. The carbon fibers are surrounded by single MT in sample C.

The PLM provided the information about the texture on a coarse scale. For analyzing the microstructures close to the F/M interface in more detail, TEM and HRTEM with SAED were used in this study. Figure 2 shows the TEM micrographs of the F/M interface and the SAED patterns of the matrix in the as-received composites. In Fig. 2a, the OA of $23° \pm 2°$ corresponds to HT pyrocarbon matrix and the inserted SAED pattern illustrates the high degree of parallel alignment of the (002) basal planes in HT matrix. Moreover, it can be seen that the HT layer contains numerous microcracks, which are approximately parallel to one another and oriented parallel to the fiber surface. Owing to the weak vander Waals forces between layers, microcracks are easily induced in HT matrix during the course of mechanically thinned and ion milling. However, no microcracks are displayed in the interface of the fiber–HT matrix. It demonstrates that there is a relatively good adhesion between the fiber and HT matrix. In Fig. 2b, c, the inserted SAED patterns and the corresponding OA angles indicate two quite different textures, i.e., LT matrix, OA $= 105° \pm 2°$ and MT matrix, OA $= 65° \pm 2°$. In contrast to HT matrix, there are not any cracks within LT and MT matrix in the vicinity of the fiber surface. It can be seen that the LT and MT are composed of particles with different sizes and shapes. These particles are cross-linked to form mosaic-like texture. Furthermore, few microcracks can be detected in the interface of the fiber–LT matrix. Reznik and Gerthsen [17] also observed that the cracks are generated not directly at the fiber–LT matrix interface but

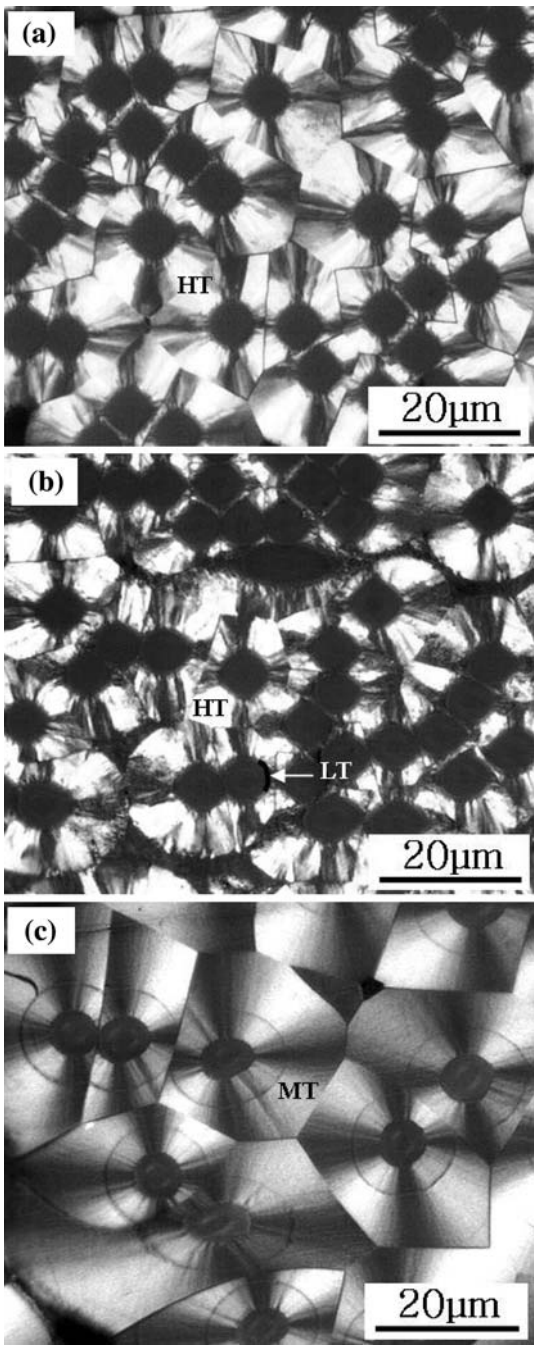

Fig. 1 Polarized light micrographs of **a** sample A; **b** sample B; **c** sample C

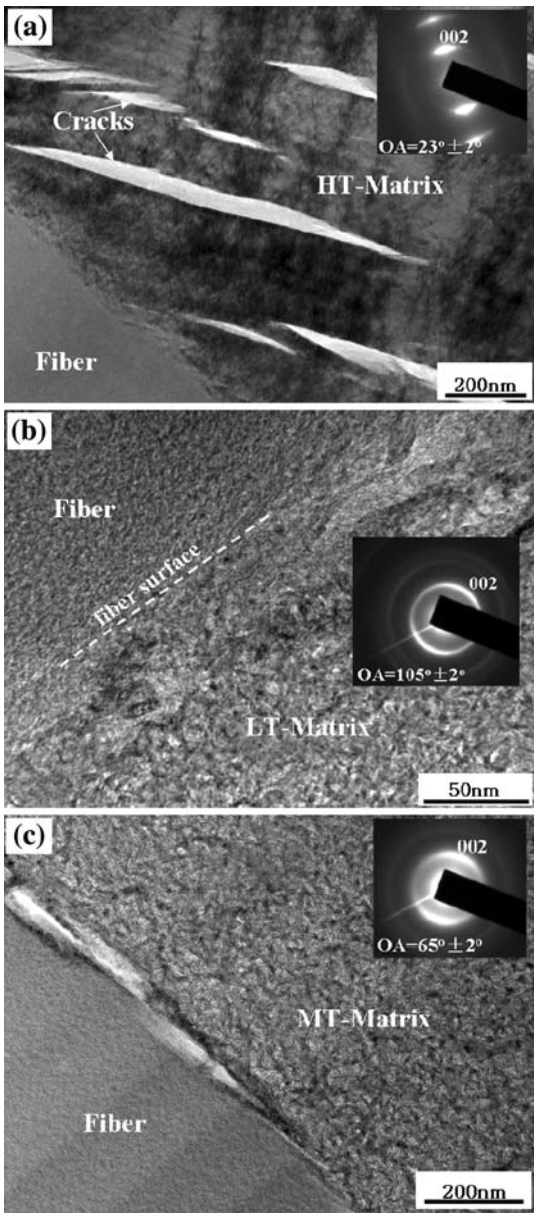

Fig. 2 TEM micrographs of the fiber/matrix interface in the 2D C/C composites **a** sample A; **b** sample B; **c** sample C. Inserts correspond to SAED patterns of the pyrocarbon matrix

at some distance in the LT matrix. These observations are indicative of a strong adhesion between the fiber and LT matrix. Figure 2c indicates that there is a microcrack between the fiber and MT matrix, which is produced by heat treatment. However, the microcrack does not spread throughout the fiber surface.

Figure 3 displays the HRTEM micrographs of the F/M interface region of 2D C/C composites. It should be noted that there are obviously different interface microstructures between the fibers and HT, LT, and MT, respectively. Figure 3a reveals that the highly ordered graphene layers exhibit long-range order and parallel to the fiber surface in the HT matrix. The 002 lattice fringes are curved to some extent in about 5-nm interface region of the fiber–HT matrix. These curved lattice fringes may be produced by stress or they replicate the unevenness of the fiber surface. Therefore, debonding cannot probably take place between the fiber and HT matrix in the course of mechanically thinned and ion milling. It is clear in Fig. 3b that some globular particles about a few nm are first formed on the fiber surface. The following is the HT layer of up to 10 nm

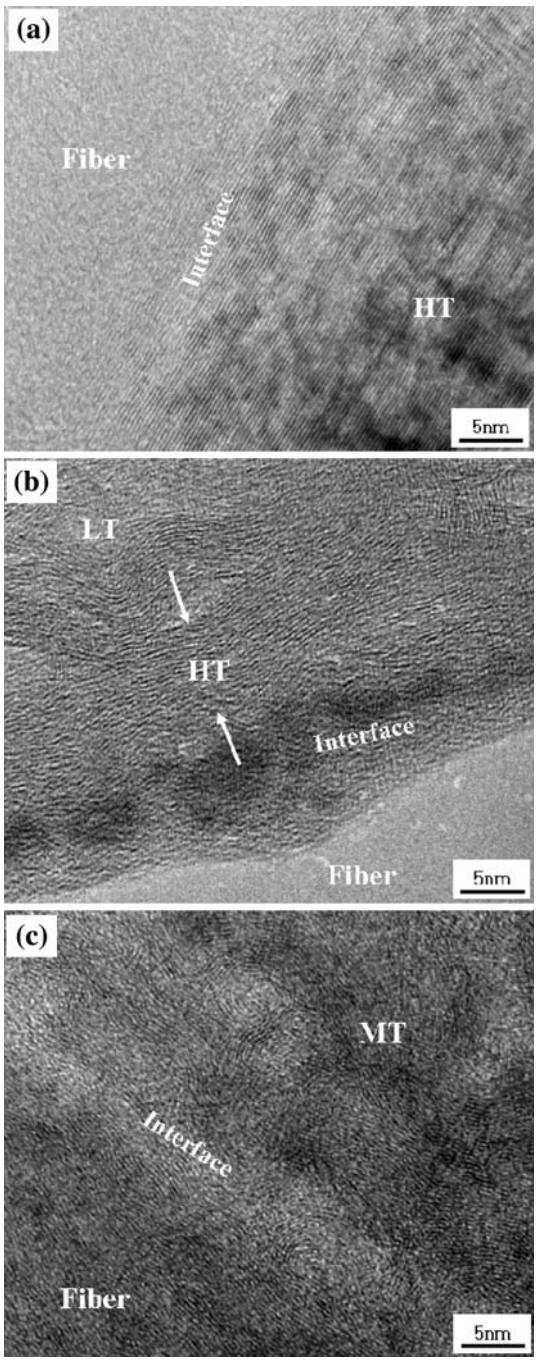

Fig. 3 HRTEM micrographs of the fiber/matrix interface **a** the fiber–HT interface in sample A; **b** the fiber–LT interface in sample B; **c** the fiber–MT interface in sample C

and the next layer is LT matrix. The globular particles possibly nucleate directly at active sites on the fiber surface and grow up gradually in the following deposition. The polyhedral particles forming LT matrix exhibit oriented graphite-like shells and a relatively disordered central part. In regard to the forming of HT layer on a scale of a few nanometers, Gerthsen et al. [18] also observed similar highly oriented layers in the interface of fiber–LT matrix and proposed stress-induced ordering mechanism. The detailed mechanism of the generation of such layer is not clear yet at present. Nevertheless, the ordered graphene layers of the shells of LT particles should be helpful to the formation of the thin HT layer. It can be concluded that a considerably strong adhesion between the fiber and LT matrix is achieved. The contact area microstructure of the interface region between the fiber and MT matrix is shown in Fig. 3c. It can be seen that in the vicinity of the PAN carbon fiber surface contains extended domains of stacked graphene layers which are often oriented parallel to the fiber surface. Meanwhile, the graphene layers stacks are scrolled and folded in the MT matrix. Moreover, some graphene layers in fiber and MT matrix waved together in the bonding area. They can improve the bonding force of the fiber with MT matrix like a hook. Therefore, the interfacial bonding force of the fiber–MT matrix is very strong.

Fracture behavior of the 2D C/C composites

The typical nominal stress–strain curves of the investigated samples A–C are shown in Fig. 4. It can be seen from the curves that samples A and B exhibit pronounced pseudo-plastic fracture behavior, while sample C experiences a brittle fracture behavior. Sample C possesses the highest flexural strength. Samples A and B have the lowest and medium flexural strength, respectively. SEM micrographs of fracture surface of the samples after three-point bending tests are demonstrated in Fig. 5. A larger extent of fiber-pullout in samples A and B agrees with the pseudo-plastic fracture behavior. Less obvious fiber-pullout proves the brittle fracture behavior of sample C. In addition, Fig. 6

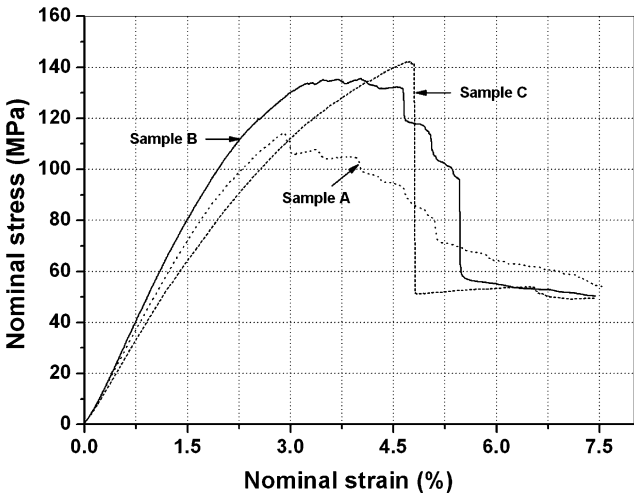

Fig. 4 Typical nominal stress–strain curves of the 2D C/C composites

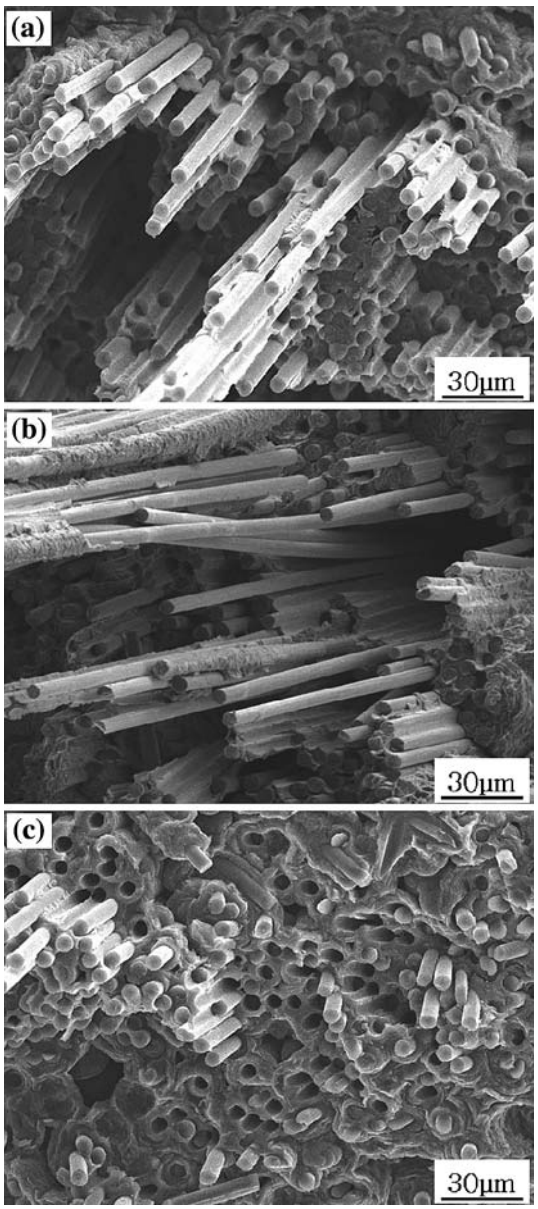

Fig. 5 SEM micrographs of fracture surface of the samples after three-point bending tests **a** sample A; **b** sample B; **c** sample C

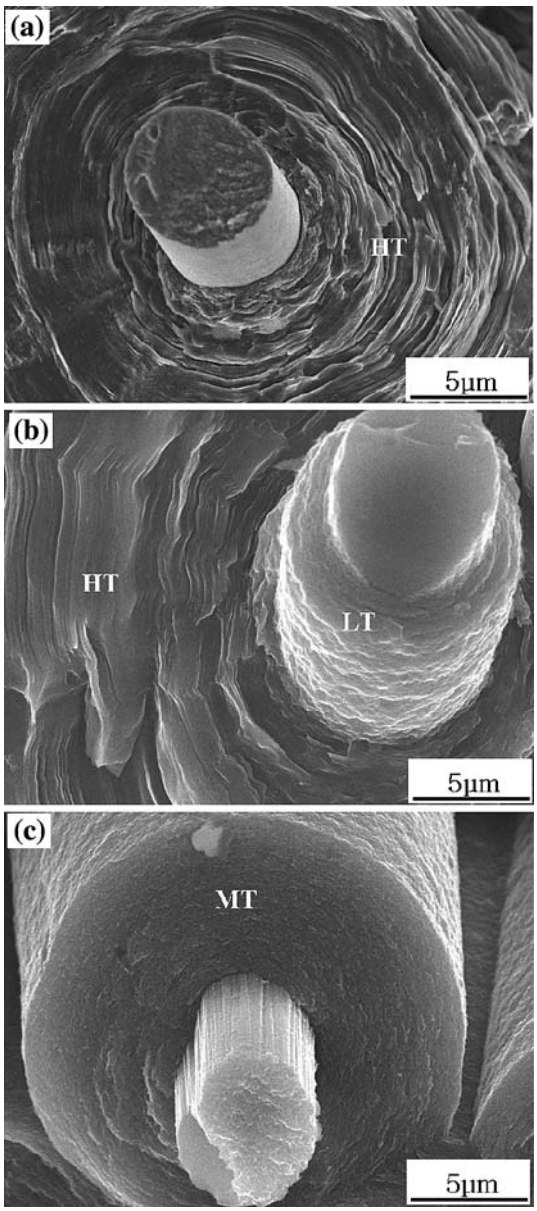

Fig. 6 SEM micrographs of fracture surface of the different pyrocarbon matrices **a** HT; **b** HT and LT; **c** MT

shows the SEM micrographs of fracture surface of the different pyrocarbon matrices in samples A–C. In Fig. 6a, b, a stepwise morphology and relative rough fracture surface are observed in HT layers. The HT layer exhibits an intensive fragmentation of kinked sublayers. From Fig. 6b, we can see that the fiber and its vicinal LT pyrocarbon layers suffer from fracture in the same plane. As a result, they are pulled out together from HT layers. Figure 6c demonstrates that the fracture surface of MT layers is a very smooth plane which is vertical to the fiber surface.

The fracture behavior of 2D C/C composites is determined by the matrix texture and the F/M interface in the composites. The experimental results show that the cracking occurs mainly within HT carbon layers and less frequently in MT and LT carbon layers. The rough fracture surface of HT matrix proves that a multiple crack deflection takes place in HT layers leading to energy dissipation, which makes contribution to the toughness enhancement. In sample A with pure HT matrix, the crack propagation is blocked by the curved graphene layers on the fiber surface. The debonding generates not directly at the F/M interface but in the highly ordered graphene layers. The pseudo-plastic fracture behavior of sample A can be ascribed to the pure HT layer matrix and a comparatively moderate interfacial bonding force. The globular particles growing at active sites on the fiber surface and thin HT layer

originating from LT matrix make the fiber and LT matrix adhere closely. The microcracks from the outer layer HT matrix take place defection at the LT–HT interface. They propagate along the surface of LT matrix, and thus the sliding is brought out between the LT and HT matrix. Therefore, the toughness fracture behavior of sample B is caused by the dominant HT layer and the interfacial sliding between different texture matrices. Both a strong adhesion of the fiber–LT matrix and the thicker fiber increased by surrounding LT pyrocarbon result in the increasing of flexural strength. Owing to the mutual winding of graphene layers in the F/M interface and MT matrix, the defection and propagation of the cracks become very difficult. Consequently, sample C experiences a brittle fracture behavior and possesses the highest flexural strength.

Conclusions

The interface microstructures of the fiber–HT, –LT, and –MT matrices are obviously different. The highly ordered graphene layers exhibit parallel to the fiber surface in HT matrix. The microcracks are not produced in the interface of the fiber–HT matrix, but in HT matrix. Some globular particles on a scale a few nanometers exist at the interface of the fiber–LT matrix. An HT layer of about 10 nm is formed before LT deposition. The graphene layers in fibers and MT matrix are waved together in the bonding area, which can improve the bonding force of the fiber–MT matrix.

The pseudo-plastic fracture behavior of the 2D C/C composites resulted from the dominant HT matrix and a comparatively moderate interfacial bonding force. A strong adhesion of the fiber–LT matrix and the thicker fiber increased by surrounding LT layers result in the increasing flexural strength. The single MT matrix and a very strong bonding force of the fiber–MT matrix lead to a brittle fracture behavior.

Acknowledgments The authors thank the financial support from the National Natural Science Foundation of China (No. 90716024) and the "111" Project (No. B08040).

References

1. Fitzer E, Manocha LM (1998) Carbon reinforcements and carbon/carbon composites. Springer, Berlin
2. Li HJ, Li AJ, Bai RC, Li KZ (2005) Carbon 43:2937
3. Benzinger W, Hűttinger KJ (1999) Carbon 37:931
4. Hu ZJ, Zhang WG, Hűttinger KJ, Reznik B, Gerthsen D (2003) Carbon 41:749
5. Zhang WG, Hűttinger KJ (2003) Carbon 41:2325
6. Tang SF, Deng JY, Liu WC, Yang K (2006) Carbon 44:2877
7. Li XT, Li KZ, Li HJ, Wei J, Wang C (2007) Carbon 45:1662
8. Tezcan J, Ozcan S, Gurung B, Filip P (2008) J Mater Sci 43:1612. doi:10.1007/s10853-007-2333-z
9. Lavenac J, Langlais F, Féron O, Naslain R (2001) Compos Sci Technol 61:339
10. Lee JY (2005) J Mater Sci 40:3573. doi:10.1007/s10853-005-2884-9
11. Guellali M, Oberacker R, Hoffmann MJ (2005) Carbon 43:1954
12. Xu GZ, Li HJ, Bai RC, Wei J, Zhai YQ (2008) Mater Sci Eng A 478:319
13. Chen TF, Reznik B, Gerthsen D, Zhang WG, Hűttinger KJ (2005) Carbon 43:3088
14. Li HL, Xu GZ, Li KZ, Wang C, Li W, Li ML (2009) J Mater Sci Technol 25:109
15. Bourrat X, Trouvat B, Limousin G, Vignoles G, Doux F (2000) J Mater Res 15:92
16. Reznik B, Hűttinger KJ (2002) Carbon 40:621
17. Reznik B, Gerthsen D (2003) Carbon 41:57
18. Gerthsen D, Bach D, Pauw VD, Kalhöfer S, Reznik B, Send W (2006) Int J Mater Res 97:1052